



Keywords

Bubble Point Test,
Membrane Characterisation,
Track-Etched Membrane,
Pore Size and Pore Size
Distribution

Received: July 19, 2014

Revised: July 25, 2014

Accepted: July 26, 2014

The use of bubble point test in membrane characterisation

I. M. T. A. Shigidi^{1,2}

¹Department of Chemical Engineering, College of Engineering, King Khalid University, P.O. Box 9036. Abha 61413, Kingdom of Saudi Arabia

²Department of Chemical Engineering, Faculty of Engineering, Al-Neelain University, P.O. Box 10179. Khartoum, Sudan

Email address

etaha@kku.edu.sa

Citation

I. M. T. A. Shigidi. The Use of Bubble Point Test in Membrane Characterisation. *American Journal of Science and Technology*. Vol. 1, No. 4, 2014, pp. 140-144.

Abstract

The use of the bubble point test was investigated in defining track etch membranes characteristics. The method applied monitors the gas-liquid interfacial interaction as the gas penetrates the wetted membrane, thus expels the wetting liquid from the pores. Relationships were based on the notion of capillary pressure, as presented in Washburn equation to relate the applied pressure to the corresponding pore's diameter. Calculations were based on the assumption of perfect cylindrical shapes of the pores as presented by the SEM pictures taken for nuclepore track-etched membranes. Results obtained were in good agreement with the manufacturers rating, hence proving reliability in using the bubble point test in assessing membrane's pore diameters.

1. Introduction

Filtration is one of the well-known conventional techniques of physical separations ever applied in chemical engineering. It has broad applications industrially and the main objectives of applying it can either be clarification of liquor purification [1], separation of solid for recovery or improving other plant operations. The filter media is the main tool playing the active role in the filtration process, so the obvious first test before applying any filter medium is to characterise it in order to define its operational capabilities.

Characterisation data for porous membranes often gives rise to misunderstanding and misinterpretations. It is not unreasonable that it is mainly the size of the pores that determine which solute can pass or which will be retained. Characterising membranes defines various parameters, that includes but not limited to; maximum, mean, minimum pore size, pore size distribution; etc. [2,3]. Another important factor is the shape of pore or its geometry; due to the complexity of combining the geometrical aspects to physical equations, to simplify the problem assumptions were made for standard geometries of pores.

There are several independent techniques for determining pore statistics [4,5,6,7,8,9,10]. A comparison summary is in table (1):

2. Materials and Equipment

2.1. Materials

Membrane filters are generally rated as absolute media. They can be

manufactured of various polymeric materials, metals and ceramics. Nominal media includes filters made of glass fibres, polymeric fibres, discrete particles (diatomaceous earth), ceramics, etc. [11]. However, even absolute media can be considered absolute only within a finite time span because of the possibility of various damage occurrence.

Figure 1 shows a scanning electron micrograph of the surface of nuclepore track etched membranes. This membrane has nearly perfect round cylindrical pores, more or less normal to the surface of the membrane, with even

random pore dispersion over the surface. Track etched membranes are absolute and are commercially available in thin films of poly-carbonate and polyester. They are manufactured in a two steps; nuclear track and etch process[10].

- In the first step, thin plastic film is exposed to ionising radiation forming damage tracks.
- In the second step, the tracks are preferentially etched out into pores by a strong alkaline solution.

Table 1. advantages and disadvantages of various membrane characterising techniques.

No.	Monitoring Technique	Advantages	Disadvantages
1	Particle counting	Continuous on-line measurements, measures several size ranges	High cost, indirect measurement of membrane integrity, may require several sensors for large scale applications
2	Particle monitoring	Continuous on-line measurement, low cost	Does not count particle size ranges, may require several sensors for large scale applications
3	Turbidity monitoring	Extensive water industry applications, low cost	Not sensitive at low turbidity, indirect method for monitoring integrity
4	Air-pressure testing	Built into membrane system, direct measuring method of integrity	Not a continuous monitoring system
5	Bubble point testing	Direct monitoring method for integrity	Must be conducted manually, labour intensive for large plants
6	Sonic sensors	Direct method, quick and easy to use	Not continuous, labour intensive for large scales.

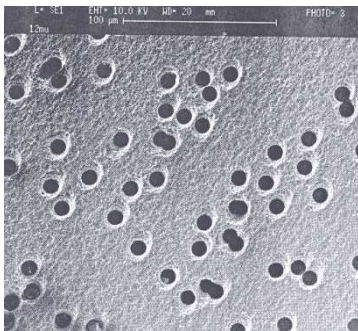


Figure (1). Nuclepore track-etch membrane filters

$$P = \frac{4\gamma \cos \theta}{D} \tag{1}$$

where P is the pressure, D diameter of capillary or pore, θ is the contact angle between the liquid and capillary wall and γ is the surface tension of the liquid.

If the liquid wets the capillary it has zero contact angle [15,16,17], therefore $\cos\theta$ can be assumed to unity, thus the equation becomes:

$$r = \frac{\gamma}{P} \tag{2}$$

2.2. POROMETERS

Many equipment have been developed and modified for characterising and measuring the integrity of microfiltration membranes; among those the Coulter Porometer manufactured by Coulter Electronics Ltd, and the PMI Porometer from Porous Material Inc., USA. Both equipment have the same operating principles whereas during experiments the sample is wetted using Gal-wick wetting agent manufactured by Porous Material Inc., USA.

2.3. Experimental Procedure

The porometer is based on the principles of capillary rise. When a capillary tube is immersed in a liquid, because of the surface tension of the liquid, the liquid is drawn up the capillary until equilibrium is established with the force of gravity [12,13,14]

The equilibrium condition can be expressed in the Washburn equation presented in the formula:

The operating mechanism depends on exposing the wetted sample to an incrementally increasing pressure applied by compressed air source. While the pressure is increasing, it reaches a point where it is enough to overcome the surface tension of the liquid in the largest pore [18,19,20]. The liquid is then rejected from the pore. Simultaneous measurements of pressure and flow are taken and when airflow and the pressure becomes linear all the pores are then opened.

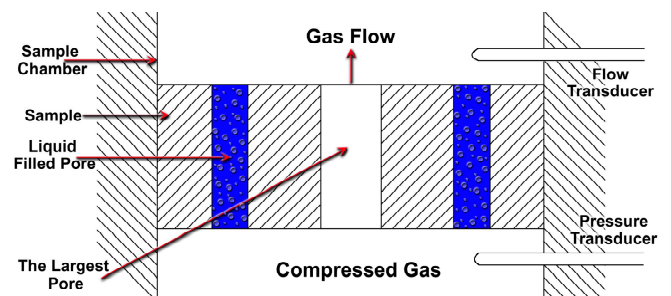


Figure (2). Schematic diagram of Porometer Chamber

The porometer monitors both pressure and flow and records these in a pressure versus flow graph for wet and dry samples figure (3). The dry data curves are determined after all the liquid has been expelled from the pores. These dry curves become the reference for calculating the pore distribution. A percentage flow distribution is calculated from the difference between wet and dry curves. If the flow is proportional to the pore area, the flow distribution can be described in terms of the pore area percentage. Assuming constant pore length, then the area distribution data will be equivalent to those of the volume distribution [21]. The square root of the area/volume values, we obtain the number distribution. Mean flow pores size (MFP) is calculated from the pressure at which the wet flow is half of the dry flow. The maximum and the minimum pore sizes are determined from the bubble point and from the point where wet and dry curves are converge.

3. Results and Discussion

Different Nuclepore track etched membranes with pore sizes of 5 μm , 12 μm , 1 μm , 0.8 μm and 0.2 μm were tested. A set of results for various pore size diameter samples are presented in the next section, before summarising the results obtained for the other pore size diameters.

Figure (3) represents a sample investigation for wet flow and dry flow for a 0.8 μm rated membrane. The half dry curve is manually calculated from the results obtained. The wet curve starts with the bubble point, which is the pore with maximum pore diameter of 1.99 μm available within the tested sample. Even though the number of pores with this diameter is considerably low giving that it only contributes to 0.17% of the air flow obtained through the tested sample, it still plays a significant role within the separation process. Such pores usually exist as a result of multiple bombardment of the same location by the activated elements as specified earlier. The increase in pressure after reaching the bubble point results in detecting more pores with smaller diameters. The flow detected at each applied pressure is always proportional to the number of pores within that particular diameter, in other words, it has been noticed from the shape of the graph the majority of pores within the tested sample are detectable with pressure between 0.45 and 0.65 bar and the results show a mean pore size for 1.14 μm . Further increase in pressure will expel more liquid and thus detect more pore diameters; this process continues till all the pores are emptied, the minimum pore detected in this case was 0.71 μm . At pressure higher than 0.8 bar the relationship between pressure and air flow is linear.

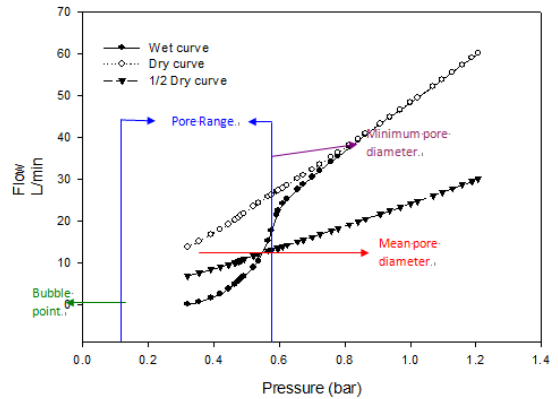


Figure (3). Wet and Dry curve for a 0.8 μm membrane

The dry curve is then produced from the dried sample using the same principle of the wet curve. The tested sample was exposed to higher pressures to ensure complete drying by reducing the limits for the minimum pore within the sample. Figure (3) shows that the pressure applied are a linear relation with the flow obtained during the dry run; that the existence of any liquid remaining within the sample reduces the linearity. The calculated half dry curve intersects with the wet curve giving the pressure required to detect the mean flow pore size of the tested sample.

The intersection of the wet curve with the dry curve occurs when all the pores are emptied, that is when the relation between the pressures applied and the flow detected became linear and the intersecting point represents the minimum pore size detected, for the 0.8 μm sample it was found to be 0.55 μm . After all the pores are empty, increasing the pressure will result in an increase of gas flow without detecting any more pores as the sample will be dry at that stage, which occurs when the wet curve meets the dry curve.

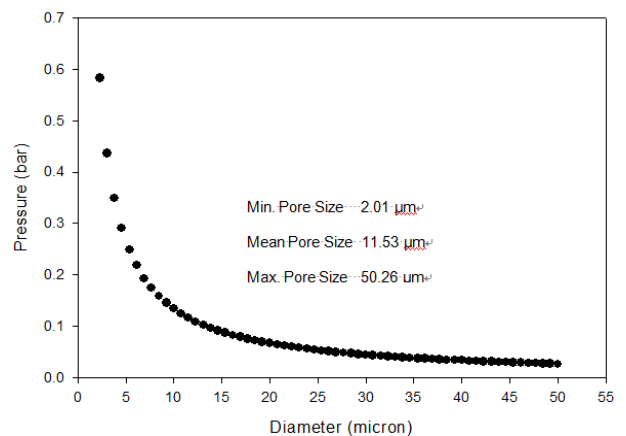


Figure (4). Pressure vs. pore diameter for 12 μm membrane sample

Figure (4) shows the relation between the detected diameters and the applied pressure for 12 μm membrane sample. This relation is governed by equation (1) and it shows the inverse proportionality between the applied pressure and the corresponding detected pores.

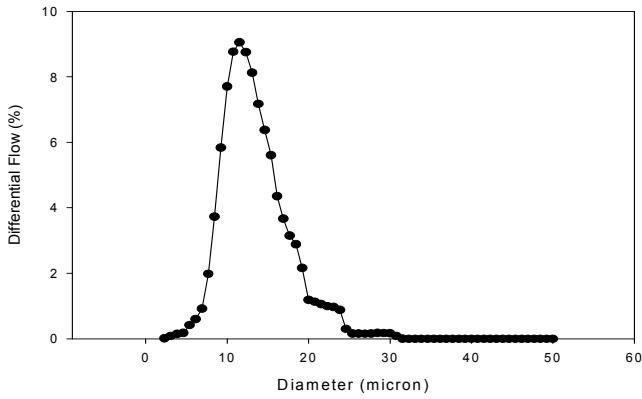


Figure (5). Differential flow percentage through a 12µm membrane

The differential flow provides the percentage of flow passing through a particular pore diameter within the tested sample, Figure (5). This information is very helpful in providing an insight about the active pore diameters within the samples, in other words, the tested sample of 12 µm may have pores with diameters of 25 µm for example, but the amount of flow passing through this size is almost negligible. This is also an indication about the pore size distribution as the presence of pores with this diameter is not common on the tested sample.

The porometer also provides the relationship between the sample's pore diameters and the cumulative flow percentage, Figure (6). This indicates the percentage amount of flow passing through the sample over the maximum to a particular pore diameter. From Figure (6) it has been noticed that the cumulative flow through the sample increases sharply between 9 µm and 15 µm pore diameters, this indicates a majority of pores within the tested sample at this range for a nominal sample of 12µm membrane rated.

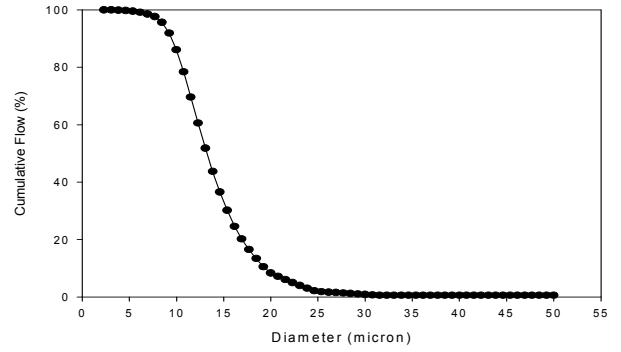


Figure (6). Cumulative pore flow for 12 µm sample

The differential pore numbers, Figure (7), shows the number of pores available within a particular diameter over a tested 25 mm diameter sample. From the cumulative flow and the differential pore number. It has been noticed that most of the air flow can be obtained between pore diameters ranging from 7 µm to 12.5 µm for the 12 µm nominal rated membrane sample.

As mentioned previously a wide range of membrane samples were tested. The overall summary for the membrane characterisations obtained are given in Table (2).

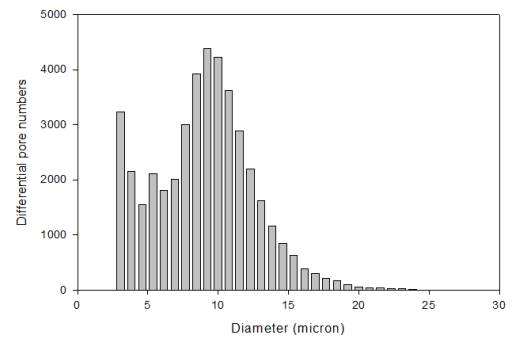


Figure (7). Differential pore diameter for 12 µm sample.

Table (2). Maximum, minimum and mean pore size diameters for different membrane samples.

Manufacturers' nominal rating (µm)	Minimum flow pore diameter (µm)	Mean flow pore diameter (µm)	Bubble point pore diameter (µm)	Error %
12	3.128	11.02	29.753	3.4
5	3.105	4.964	7.408	2.9
1	0.81	1.416	1.231	1.3
0.2	0.175	0.211	0.423	2.1

4. Conclusions

In the case on hand, the bubble point test was considered for its simplicity, non-destructive nature as well as its similarity to expose the membrane into actual operating conditions, nonetheless its ability to providing comprehensive statistical data for the specifications of the membrane under investigation. From the results obtained and presented, the bubble point test has proven reliability in specifying the minimum, mean and maximum pore sizes for the tested track etched membrane and the results obtained were in good agreement with the manufacturers

rating, in addition, the test also provided further characterising information about the pore size distribution and the differential numbers that are important in defining the membrane operational capabilities.

References

- [1] Cheremisinoff Paul, N. (1995). Solids/liquids separation. Lancaster, Pa., Technomic
- [2] Calvo, J. I., A. Hernandez, et al. (1995). "Pore Size Distributions in Microporous Membranes: I. Surface Study of Track-Etched Filters by Image Analysis." Journal of Colloid and Interface Science 175(1): 138-150.

- [3] Calvo, J. I., A. Hernandez, et al. (1995). "Pore Size Distributions in Microporous Membranes II. Bulk Characterization of Track-Etched Filters by Air Porometry and Mercury Porosimetry." *Journal of Colloid and Interface Science* 176(2): 467-478.
- [4] Capannelli, G., F. Vigo, et al. (1983). "Ultrafiltration membranes -- characterization methods." *Journal of Membrane Science* 15(3): 289-313.
- [5] Gomez Alvarez-Arenas, T. E. (2003). "Air-coupled ultrasonic spectroscopy for the study of membrane filters." *Journal of Membrane Science* 213(1-2): 195-207.
- [6] Baltus, R. E. (1997). "Characterization of the pore area distribution in porous membranes using transport measurements." *Journal of Membrane Science* 123(2): 165-184.
- [7] Hernandez, A., J. I. Calvo, et al. (1996). "Pore size distributions in microporous membranes. A critical analysis of the bubble point extended method." *Journal of Membrane Science* 112(1): 1-12.
- [8] Ju Youn, I., J. Jeong, et al. (1998). "Light transmission study for determination of pore size distribution in microporous membranes." *Journal of Membrane Science* 145(2): 265-269.
- [9] Martinez-Diez, L., F. J. Florido-Diaz, et al. (2000). "Characterization of Hydrophobic Microporous Membranes from Water Permeation." *Separation Science and Technology* 35(9): 1377-1390.
- [10] Reutov, V. F., S. N. Dmitriev, et al. (2003). "Transmission electron microscopy porometry of etched pore channels in track membranes." *Nuclear Instruments and Methods in Physics Research Section B: Beam Interactions with Materials and Atoms* 201(3): 460-464.
- [11] Venkataraman, K., W. T. Choate, et al. (1988). "Characterization studies of ceramic membranes. A novel technique using a coulter(R) Porometer." *Journal of Membrane Science* 39(3): 259-271.
- [12] Jakobs, E. and W. J. Koros (1997). "Ceramic membrane characterization via the bubble point technique." *Journal of Membrane Science* 124(2): 149-159.
- [13] Wo, S., X. Xie, et al. (2001). "A statistical model of apparent pore size distribution and drainage capillary pressure." *Colloids and Surfaces A: Physicochemical and Engineering Aspects* 187-188: 449-457.
- [14] Wo, S., X. Xie, et al. (2001). "A statistical model of apparent pore size distribution and drainage capillary pressure." *Colloids and Surfaces A: Physicochemical and Engineering Aspects* 187-188: 449-457.
- [15] Gumi, T., M. Valiente, et al. (2003). "Characterization of activated composite membranes by solute transport, contact angle measurement, AFM and ESR." *Journal of Membrane Science* 212(1-2): 123-134.
- [16] Kwok, D. Y., C. N. C. Lam, et al. (1998). "Measuring and interpreting contact angles: a complex issue." *Colloids and Surfaces A: Physicochemical and Engineering Aspects* 142(2-3): 219-235.
- [17] Marmur, A. (1996). "Equilibrium contact angles: theory and measurement." *Colloids and Surfaces A: Physicochemical and Engineering Aspects* 116(1-2): 55-61.
- [18] McGuire, K. S., K. W. Lawson, et al. (1995). "Pore size distribution determination from liquid permeation through microporous membranes." *Journal of Membrane Science* 99(2): 127-137.
- [19] Mey-Marom, A. and M. G. Katz (1986). "Measurement of active pore size distribution of microporous membranes - a new approach*1." *Journal of Membrane Science* 27(2): 119-130.
- [20] Mietton-Peuchot, M., C. Condat, et al. (1997). "Use of gas-liquid porometry measurements for selection of microfiltration membranes." *Journal of Membrane Science* 133(1): 73-82.
- [21] Troger, J., K. Lunkwitz, et al. (1998). "Determination of the surface tension of microporous membranes using wetting kinetics measurements." *Colloids and Surfaces A: Physicochemical and Engineering Aspects* 134(3): 299-304.